DOI: 10.3901/CJME.2015.0504.066, available online at www.springerlink.com; www.cjmenet.com; www.cjme.com.cn

Thrust and Torque Characteristics Based on a New cutter-head Load Model

LIU Jianqin*, REN Jiabao, and GUO Wei

Key Laboratory of Mechanism Theory and Equipment Design of Ministry of Education, Tianjin University, Tianjin 300072, China

Received September 18, 2014; revised April 28, 2015; accepted May 4, 2015

Abstract: Full face rock tunnel boring machine(TBM) has been widely used in hard rock tunnels, however, there are few published theory about cutter-head design, and the design criteria of cutter-head under complex geological is not clear yet. To deal with the complex relationship among geological parameters, cutter parameters, and operating parameters during tunneling processes, a cutter-head load model is established by using CSM(Colorado school of mines) prediction model. Force distribution on cutter-head under a certain geology is calculated with the new established load model, and result shows that inner cutters bear more force than outer cutters, combining with disc cutters abrasion; a general principle of disc cutters' layout design is proposed. Within the model, the relationship among rock uniaxial compressive strength(UCS), penetration and thrust on cutter-head are analyzed, and the results shows that with increasing penetration, cutter thrust increases, but the growth rate slows and higher penetration makes lower special energy(SE). Finally, a fitting mathematical model of ZT(ratio of cutter-head torque and thrust) and penetration is established, and verified by TB880E, which can be used to direct how to set thrust and torque on cutter-head. When penetration is small, the cutter-head thrust is the main limiting factor in tunneling; when the penetration is large, cutter-head torque is the major limiting factor in tunneling. Based on the new cutter-head load model, thrust and torque characteristics of TBM further are researched and a new way for cutter-head layout design and TBM tunneling operations is proposed.

Keywords: TBM(full face rock tunnel boring machine), cutter-head load model, CSM(Colorado school of mines) model, cutter-head layout design,thrust and torque

1 Introduction

Full face rock tunnel boring machine has been widely used in hard rock tunnels, urban underground rail, coal and other full-face tunnels, and there are many well-known full face rock tunnel boring machine(TBM) manufacturers worldwide, such as Herrenknecht and Robbins, however, the TBM design criterion is not clear yet, and technicians' experience plays an important role in design. In this paper, some key factors that influence forces on the cutter-head are analyzed and some design criteria are proposed for cutter-head layout design and TBM tunneling operations.

With dozens of disc cutters arranged on it, cutter-head is one of the most important components on TBM. The structure of disc cutter, geological parameters, and operating parameters determine the force on cutter. Arrangement of cutters on the cutter-head influences tunneling process and load transferring rules. The cutter-head load model will be more complicated under different geological and operating parameters, so it is necessary to study relationship among them to provide theoretical basis for TBM design and to select proper operating parameters in boring processes. The theory of rock fragmentation is the basis of the cutter-head load model. Rostami put forward Colorado School of Mines(CSM) force prediction model[1] based on linear cutting machine(LCM), one of the most commonly used formulas. Based on CSM cutter force prediction model, LI, et al, predicted cutters wear and special energy[2–3], and the results indicated that the model can not only predict real-time specific energy for cutter-head, but also provide a theoretical basis for the performance prediction and optimal design of cutter-head for TBM. Professor ZHANG, et al, put forward a balancing theory of forces acting on cutter-head of TBM during rock breaking and set up a mathematical mechanical model of disc cutter layout[4], HUO, et al, presented a nonlinear multi- objective disc cutters' layout mathematical model with complex constraints and the corresponding multi-stage solution strategy, in which the whole disc cutters' layout design process was decomposed into the disc cutters' spacing design and the disc cutters' plane layout design[5–6]. Cutters' life plays an important role in cutter-head design theory. ZHANG, et al, put forth a new method concerning prediction of life span and wear of TBM disc cutters, as well as timing for replacing disc cutters[7–8]. GUO, et al,

* Corresponding author. E-mail: liujianqin@tju.edu.cn

Supported by National Natural Science Foundation of China(Grant No. 51275339), and National Basic Research Program of China(973 Program, Grant No. 2013CB035402)

analyzed that the cutter-head open ratio and its opening distribution characteristics design influenced the efficiency of shield tunneling[9–10]. SAFFET analyzed data from the Queen of Water Tunnel and put forward a driving speed prediction model under different joints[11]. ROSTAMI, et al, compared two of the most successful performance prediction models, namely CSM and the Norwegian Institute of Technology(NTH) model, and analyzed their shortness and strength[12].

Researches stated above are on the basis of the CSM model. Some papers analyzed the effect of operation parameters on the efficiency of the tunneling, and some were about cutter-head layout design with optimization goal of minimize overturning moment to optimize the design of the cutter head. There are few published papers in literatures on force distribution on cutter-head, and cutter abrasion is not considered during cutter-head layout optimization. Few studies have been done about thrust and torque on the cutter-head for hard rock tunnel boring machine in complex geological environment. Key parameters are extracted in geological parameters, operating parameters and cutter parameters based on existing force prediction model in the present paper. A new cutter-head load model including geological parameters, cutter parameters and operating parameters is established. Within this model, force distribution on the cutter-head under certain geological conditions is analyzed; according to the analysis of the force distribution on cutter-head and cutter abrasion, a general principle of disc cutters' layout design is proposed. It is analyzed the influence of geological and tunneling parameters on thrust and torque on the cutter-head, and the results are compared with recorded data from Qingling tunnel to verify the correctness and feasibility of the load model. Finally, the relationship between ZT(the ratio of torque and thrust) and penetration depth is studied, and a mathematical fitting model is established, which is helpful for selecting proper tunneling parameters for efficient tunneling process.

2 Mathematical model

2.1 Extract key parameters

There are many researches about what factors impact the forces on cutters. A simple mathematical model is proposed, on which the evidence of experimental data is found to provide a good description of the magnitude and variation of the thrust and rolling forces with disc diameter edge angle and penetration by ROXBOROUGH and PHILLIPS[13]. Based on a simplified theoretical analysis and the experimentally proven assumption by SANIO, tensile rather than shear failure is the dominant for rock breaking, I_{s50} is defined as the parameter to represent the strength of rock[14]. ROSTAMI's research shows that rock's uniaxial compressive strength, tensile strength, cutter's geometry, and penetration depth influence the forces on cutters[1]. Research by XIA, et al shows that both phase difference and the installation radius between adjacent disc cutter have little effect on the normal force and the rolling force[15].

In the existing commonly used force prediction model, parameters are generally divided into three categories. The first category is geological parameters, which reflect the difficulty in the cutter breaking rock, such as UCS, tensile strength, and shear strength. The second category is cutter parameters, which reflect cutter geometry and cutter spacing such as cutter's radius and tip width thickness. The third category reflects rock fragmentation process, known as tunneling parameters, such as penetration p and cutter rotation speed ω. Part of parameters used in commonly used cutter force prediction models are listed in Table 1.

Table 1. Parameters used in commonly used cutter force prediction models

Classification	Commonly models	CSM model
Geological	σ_t, σ_c, τ, I_s, Q_d, S_{20}, C_r	σ_t, σ_c
Cutter	R, T, α, S, D_m, n	R, T, S
Tunneling	p, ω	p

σ_c—Uniaxial compressive strength(UCS),
σ_t—Brazilian tensile strength of rock,
τ—Shear strength,
Q_d—Rock quality designation,
C_r—Rock fracturing class,
I_s—Point load index,
S_{20}—Brittleness index,
R—Cutter radius,
T—Cutter tip thickness,
α—Tip angle,
S—Cutter spacing,
p—Penetration,
ω—Rotation speed of cutter-head,
D_m—Diameter of cutter-head,
n—number of cutters on the cutter-head.

Table 1 shows the parameters used in common models focus on cutter size and geological conditions, due to most all cutter force prediction models are based on linear cutting, ignoring the cutters' location on cutter-head, so installation phrases are neglected in the new established model. Q_d and Rock Class are represented by σ_c and σ_t, because UCS and Brazilian tensile strength of rock can reflect the cracks and joints in the rock. Installation radius is represented by spacing between cutters. Number of cutters in the cutter-head and machine diameter are included in new load model. Rotation speed of cutter-head can be neglected when the cutter-head rotated at a low speed. The cutter-head load model focuses on the force distribution on cutter-head with different cutters arrangements, and torque characteristics on cutter-head at different tunneling speeds. Therefore, parameters were reselected for cutter-head load model. Parameters used in cutter-head load prediction model are listed in Table 2. With this model, this paper will focus on load distribution on cutter-head in particular geological condition, and the influence of tunneling parameters on thrust and torque.

Table 2. Parameters used in cutter-head load prediction model

Geological	Cutter-head	Tunneling	Load on cutter-head
σ_c , σ_t	D_m, S, n	p	F_{th}, T_{tor} , ρ

2.2 Force prediction model in different location

Fig. 1 shows disc cutter structure: D is cutter diameter, R is cutter radius, and T is cutter tip thickness. For 17-inch disc cutter, the diameter is 432 mm, and the tip thickness is 12.5 mm.

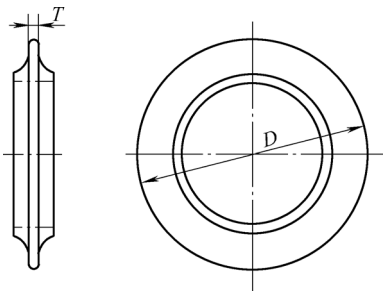

Fig. 1. Geometry of disc cutter

CSM model predicts forces when cutters broken rocks vertically, however, due to the cutters' different positions on the cutter-head, it's difficult to calculate the forces on cutter-head at one time. So we divide cutters into normal cutters and side cutters according to their position on cutter-head. The force model of differences kind of cutters are shown in Fig. 2.

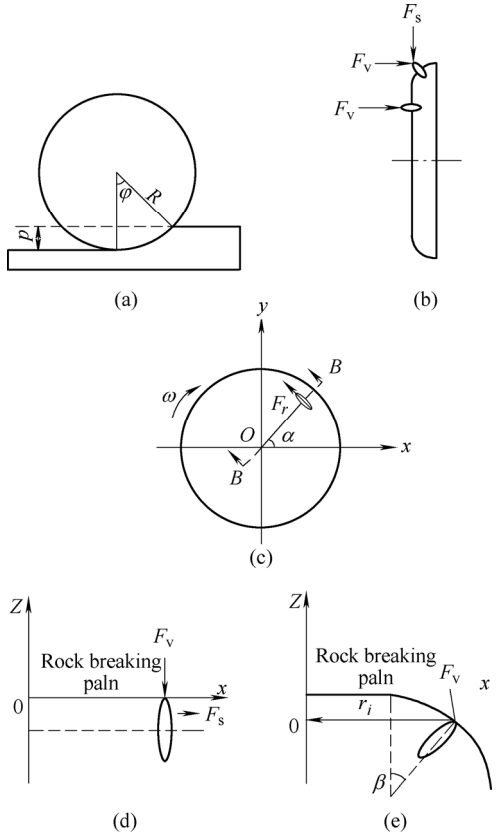

Fig. 2. Forces of cutters' on different positions on the cutter-head

Fig. 2(a) shows rock breaking model, which depicts the disc cutter penetrates the rock and forms tensile cracks. In order to estimate forces acting on the cutter-head, one should integrate all forces on normal cutters and side cutters. The region of interaction can be specified by φ, which is determined by cutter radius and penetration as follows:

$$\varphi = \arccos\left(\frac{R-p}{R}\right), \tag{1}$$

where φ—Angle of the contact area.

Fig. 2(b) shows direction of normal force and side force for normal cutters and side cutters. Fig. 2(c) shows rolling force when cutter-head rotates clockwise. It is shown that the force between the cutter and rock is decomposed into normal force, side force, and rolling force. The normal force is vertical to the working face and the rolling force is in the opposite direction of the cutter-head rotation.

In order to calculate the forces on the cutter-head, we must estimate forces on cutters first. CSM force prediction model was a theoretical/empirical model, which was developed by ROSTAMI, has been widely used in projects with great success. So, the CSM model was selected to estimate the force on each cutter. In CSM model[7], the force acting on a disc cutter was integrated force elements caused by pressure acting on disc cutter (Fig. 3), so the cutter force can be calculated as follows:

$$\mathrm{d}F = TpR\mathrm{d}\theta = TRp^0\left(1-\frac{\theta}{\varphi}\right)\mathrm{d}\theta, \tag{2}$$

where p^{θ}—Base pressure,
θ—Angle from the normal to face, range from 0 to φ.

$$F_t = p^0\varphi RT, \tag{3}$$

where F_t—Resultant force.

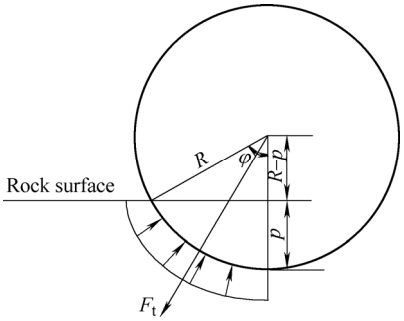

Fig. 3. Pressure distribution along the disc cutter periphery

In equations above, all variables are known except for p^0, which is a function of the cutting geometry and rock properties. For this purpose, a database of measured forces from linear cutting tests performed in the laboratory in

various rock type and using different cutting geometries has been used. The estimated P^0 is shown in Eq. (4):

$$p^0 = C\sqrt[3]{\frac{S}{\varphi\sqrt{RT}}\sigma_c^2\sigma_t}, \tag{4}$$

where p^0—Base pressure,

C—Constant for the pressure distribution function (typically 2.12 for 432 mm cutters, and increasing with the increased cutter tip width).

As shown in Fig. 2(b), normal force is vertical to the working face of the normal cutter, however the normal force on side cutter is not parallel to that of normal force. So the direction of normal force on side cutter is redefined to parallel that of normal cutter, making it easier to calculate thrust on cutter-head. Fig. 2 (d) and Fig. 2 (e) show normal force on the normal cutter and the side cutter.

$$F_v = F_t \cos\left(\frac{\varphi}{2}\right)\cos\beta, \tag{5}$$

$$F_r = F_t \sin\left(\frac{\varphi}{2}\right), \tag{6}$$

where F_v—Normal force,

F_r—Rolling force,

β—Cutter install angle.

According to Eqs. (1)–(6), normal force can be calculated for each cutter, but it is too complex for cutter-head when all cutters have the same size and similar face geology. Consequently, cutter parameters and geological parameters in the equation are separated and simplified as follows:

$$G = RT, \tag{7}$$

$$Q = \sigma_c^2\sigma_t, \tag{8}$$

$$\lambda = 2.12S^{\frac{1}{3}}, \tag{9}$$

$$F_t = \lambda G^{\frac{5}{6}} Q^{\frac{1}{3}} \varphi^{\frac{2}{3}}, \tag{10}$$

where G—Cutter coefficient, 2700 mm^2 for 432 mm cutter,

Q—Geology coefficient,

λ—Cutter arrangement coefficient.

Eq. (10) is the simplified relationship among cutter parameters, geological parameters, and forces on cutters. As all cutters on cutter-head have same size, G and Q are fixed values in certain geological coefficient.

2.3 TB880E cutter-head load model

Qinling Tunnel was the first railway tunnel constructed using TBM in China, and a gripper Wirth TB880E(see Fig. 4) was selected for the project with specifications summarized in Table 3. Cutters were placed on the cutter-head randomly, which was a common way for cutter arrangement. With the load model established above, the TB880E cutter-head load model was established, studying force distribution on cutter-head. Results were compared with engineering data to verify the accuracy of this model.

Fig. 4.　Cutter-head of TB880E

Table 3.　Design Parameters of TB880E

Parameter	Value
Cutter-head diameter D_m/m	8.800
Cutter-head power P_c/MW	3.440
Maximum torque $T_{tor\,max}$ /(MN • m)	5.800
Maximum thrust $F_{th\,max}$ /MN	21.000
Cutter diameter D_c /mm	432
Cutter-head speed ω/(rad • s^{-1})	0.565/0.283
Disc nominal spacing S/mm	65

Fig. 5 shows TB880E cutter-head layout[16]: cutter-head diameter is 8800 mm with 71 cutters, including 6 center cutters, 51 normal cutters, 12 side cutters, and 2 reaming cutters.

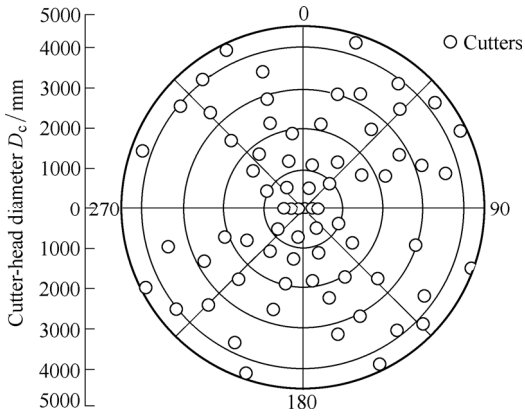

Fig. 5.　Disc cutters' layout scheme of TB880E

According to the derived force model Eqs. (7)–(10), calculate thrust and torque on the cutter-head:

$$F_{it} = \lambda_i G^{\frac{5}{6}} Q^{\frac{1}{3}} \varphi_i^{\frac{2}{3}}, \tag{11}$$

$$\varphi_i = \arccos\left(\frac{R - p_i}{R}\right), \tag{12}$$

$$F_{\text{th}}=\sum_{i=1}^{n}F_{iv}=\sum_{i=1}^{n}F_{it}\cos\left(\frac{\varphi_i}{2}\right)\cos\beta_i, \tag{13}$$

$$T_{\text{tor}}=\sum_{i=1}^{n}F_{it}\sin\left(\frac{\varphi_i}{2}\right)r_i, \tag{14}$$

where λ_i—Cutter arrangement coefficient of the ith cutter,
φ_i—Angle of the contact area for the ith cutter,
F_{th}—Thrust on the cutter-head,
T_{tor}—Torque on the cutter-head,
P_i—Penetration of the ith cutter, when several cutters are on the same track $P_i=p/n$.

The Qinling Tunnel is a long tunnel with complicated geological conditions and the rock UCS reaches up to 302.1 MPa(mostly around 130 MPa[17]). Force distribution and eccentricity on cutter-head are derived by the cutter-head load model, and results are shown in Table 4, Table 5 and Fig. 6.

$$x=\frac{\sum M_x}{F_{\text{th}}}, \tag{15}$$

$$y=\frac{\sum M_{\text{y}}}{F_{\text{th}}}, \tag{16}$$

$$\rho=\sqrt{x^2+y^2}, \tag{17}$$

$$\theta=\begin{cases}\arctan\dfrac{y}{x} & (x>0),\\ \dfrac{\pi}{2}+\arctan\dfrac{y}{x} & (x<0),\end{cases} \tag{18}$$

where M_x—Bending moment of the x axis,
M_y—Bending moment of the y axis,
ρ—Eccentricity,
θ—Eccentric angle.

Table 4. Eccentricity of cutter-head under certain geological condition

Uniaxial compressive strength σ_c /MPa	Brazilian tensile strength of rock σ_t /MPa	Eccentricity ρ/mm	Eccentric angle θ/rad
150	7.5	127	0.365

Table 5. Forces of cutters under certain geological condition

Penetration	Forces on cutters F_v/kN		Thrust
p/mm	Max	Min	F_{th}/kN
5	132	97	85 858
9	161	117	10 455
13	181	132	11 831

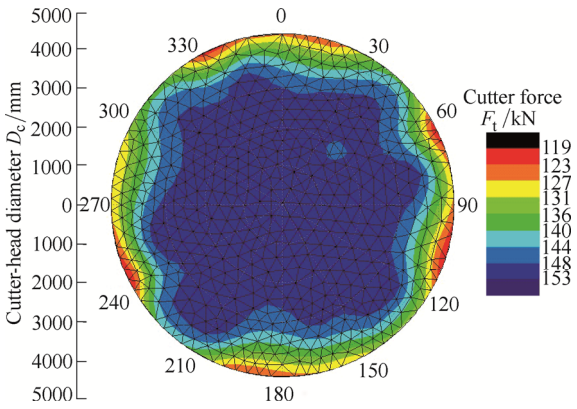

Fig. 6. Load distribution under normal load condition

Fig. 6 shows that forces on cutters in a different location on the cutter-head vary widely, forces on cutters in the center are maximal and reduce with increasing cutter installation radius. Because cutters at the center of the cutter have the same cutter spacing, the zone from 148 to 153 is larger than other zones. This is consistent with M. Entacher's study[18], shown as in Fig. 7: forces on central cutters are larger than that of side cutters.

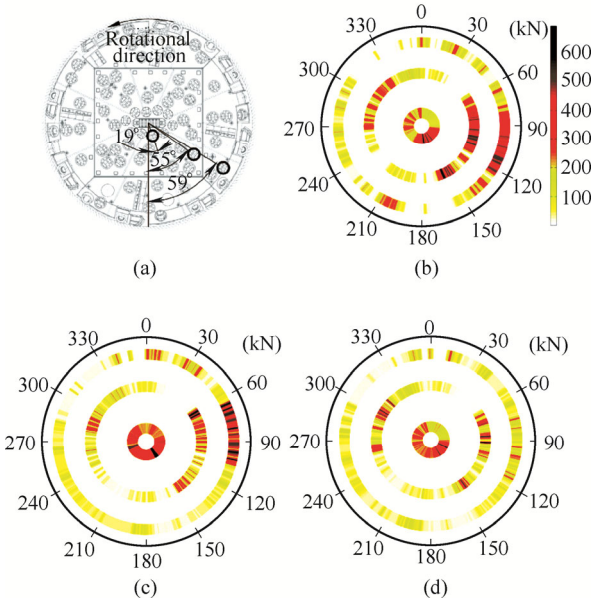

Fig. 7. F_N is cutter-head vertical force during three consecutive cutter-head revolutions measured by ENTACHER M.

$$E_{\text{s}}=\frac{E}{V}=\frac{F_{\text{th}}\times p+2\pi T_{\text{tor}}}{\pi R^2 p} \tag{19}$$

Fig. 8 shows that Specific Energy of each cutter in different locations on the cutter-head varies widely, and cutters in the center consume less energy than cutters of other zones ,which means a high efficiency to boring the rock. However, cutters in the central bear higher forces.

2.4 Principle of disc cutters' layout design

$$A_i=\pi\left(r_i^2-r^2{}_{i-1}\right)=\pi S_i(r_i+r_{i-1}), \tag{20}$$

where A_i—Rock breaking area of the ith cutter,
S_i—Spacing between the ith cutter and the one ahead;
r_i—Cutter installation radius.

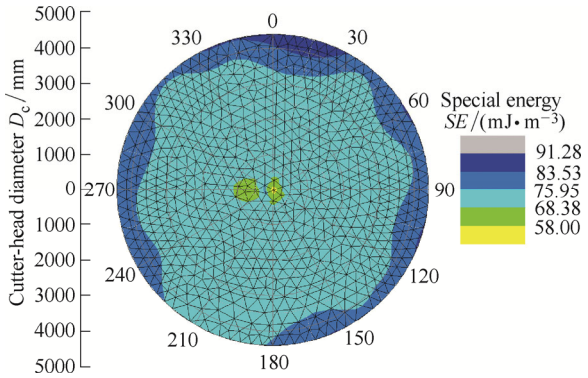

Fig. 8. *SE* distribution under normal load condition on the cutter-head

Fig. 9 shows that there is a positive correlation between cutter abrasion and rock breaking area. They both increase with cutter numbers. On the edge of cutter-head, two or three cutters were set on the same radius in order to reduce cutters' wear. At the same time, cutters at inner ring are set a broad spacing to control the total amount of cutters on the head.

$$A_i = \frac{\pi R_c^{\ 2}}{n}, \tag{21}$$

$$r_i = \sqrt{\frac{A_i}{\pi} + r_{i-1}^2}, \tag{22}$$

where R_c—Radius of cutter-head.

Spacing design for cutters in different geology has been studied by many researchers[19–21]. But they never consider cutters' position on cutter-head. Fig. 6 shows that spacing between cutters at the center of cutter-head is the largest. A_i is an empirical value relates to rock abrasion. In Eqs. (21)–(22), r_i of each cutter is determined. When the spacing between cutters is too small, we put two cutters on the same trace. In this way, the number of abnormal wear cutters reduced, and less time spent on replacing cutters.

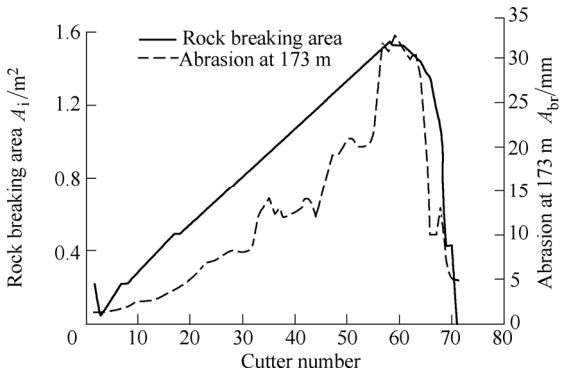

Fig. 9. Cutters' abrasion and breaking area

According to the analysis above, a new principle considering force distribution and cutter abrasion is used to solve the disc cutters' arrangement on the cutter-head. The load and the largest rock breaking spacing are the major limiting factors when cutters are arranged on the center of the cutter-head. Abrasion is the major limiting factor and outer circle cutters spacing is smaller when cutters are arranged on the outer ring cutters.

3 Characteristics of cutter-head thrust and torque

3.1 Thrust in different geological conditions

According to data in Qinling Tunnel, thrust on the cutter-head is estimated (model applied in TB880E takes σ_t:σ_c=1:20). Table 6 shows part of recorded thrust and torque data in Qinling Tunnel.

In Table 7, the force on cutters is the maximum F_v estimated on the cutter-head. As the designed capacity for 432 mm cutters is 250 kN, and the rated thrust for cutter-head is 17.3 MN, comparing with the data in Table 4, TB880E conforms to the requirements of tunneling. However, driving speed slows when rock UCS is too high for cutters to tunnel in some special complicated regions, which was consistent with site records (Table 6).

$$I_p = \frac{F_{th}}{p}, \tag{23}$$

where I_p is field penetration index(MN/mm), describing the thrust need to tunnel unit length.

As shown in Fig. 10, the thrust increases with the increase of penetration, while I_p decreases. It is shown that the pressure of unit distance needed decreases when the penetration increases. So in case of the rated power allows, larger penetration can give full play to the TBM tunneling efficiency and achieve rapid excavation.

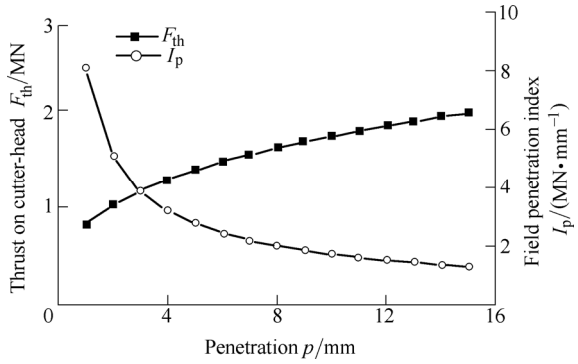

Fig. 10. Cutter force variation with penetration

SE(special energy) is an important indicator for TBM energy consumption, defining energy consumed breaking unit volume of rock.

Table 6. Part of recorded thrust and torque data in Qinling Tunnel

Data	Thrust F_{th}/kN	Torque T_{tor}/(kN • m)	Penetration p/mm	Data	Thrust F_{th}/kN	Torque T_{tor}/(kN • m)	Penetration p/mm
1	3605.3	1473.0	5.5	54	15 587.00	4649.3	8.4
2	2264.5	1402.0	5.5	55	15 228.70	4617.0	8.8
3	3444.2	1671.3	7.5	56	14 250.40	3898.2	9.8
5	9471.3	2537.6	9.3	58	15 319.70	2316.1	4.4
6	5324.7	1907.9	9.3	60	11 677.30	3288.8	10
7	13 256.00	4214.5	9.3	61	10 058.00	3182.1	10
8	13 005.40	3773.6	9.6	65	10 042.70	2999.0	12.3
9	15 519.00	4408.8	9.2	69	12 270.70	4357.3	11.3
10	15 349.80	4602.3	8.4	70	13 682.10	3327.1	9.4
11	15 129.10	4236.6	9.5	71	13 054.80	3263.8	10.3
12	15 498.10	4749.6	10.7	73	13 100.50	3915.8	10
13	15 588.00	2633.0	5.7	74	12 618.10	3626.9	9.6
14	15 871.40	3304.0	6.4	75	10 124.00	3446.5	10.2
15	13 281.10	4226.5	9.4	76	11 864.60	3888.6	10.6
16	14 122.00	4020.8	10	77	12 160.20	3515.4	9.5
17	16 336.80	3313.2	5.3	78	12 380.40	3566.9	9.7
18	13 489.00	4017.8	9.9	80	14 157.00	3922.3	9.3
19	13 923.70	4457.1	12	81	10 153.00	3064.4	9.8
20	15 480.00	4477.0	10.2	82	12 690.20	3548.9	10.3
21	15 479.00	5097.0	12.1	84	15 667.30	4129.4	9.4
22	15 273.10	3749.8	8.6	85	16 266.60	3662.0	6.3
23	15 060.50	4069.6	9.8	86	15 662.80	3197.0	5.6
27	12 171.70	3962.0	12	87	16 056.70	2902.5	4.8
28	11 740.10	3897.8	11.6	91	10 612.50	3256.5	9.6
29	15 134.50	4922.7	11	92	13 319.70	3691.3	9.6
32	10 022.90	2810.0	10.3	93	12 415.00	3638.5	9.4
33	10 178.30	2677.3	9.4	94	10 752.90	3410.5	9.5
35	11 298.50	3311.7	10.4	98	11 287.10	3366.0	9.2
36	12 852.00	3466.0	9.2	99	11 619.00	3414.1	9.3
37	13 957.60	4103.5	9.3	100	12 356.00	3499.2	9.2
38	14 949.80	4200.8	9.3	101	10 712.30	3333.5	9.0
39	12 192.20	3417.0	9.3	102	13 135.00	3883.6	9.7
40	14 420.30	3853.0	9.7	103	13 241.60	3973.1	9.8
41	16 578.90	3557.8	6.8	104	12 815.30	3113.5	7.5
42	12 452.90	3558.3	10.8	105	13 120.90	2374.9	4.3
44	10 946.40	3336.6	11.6	106	12 468.60	2506.3	4.8
45	12 155.10	3948.1	12	107	14 082.00	2671.4	5.5
46	15 131.20	4916.3	10.9	108	14 179.90	2316.0	3.9
47	13 952.20	4574.5	10.9	109	14 184.00	3951.5	9.2
39	12 192.20	3417.0	9.3	111	11 424.10	3191.5	9.6
40	14 420.30	3853.0	9.7	112	10 545.00	2976.3	8.5
41	16 578.90	3557.8	6.8	113	11 805.30	3372.3	9.6
42	12 452.90	3558.3	10.8	115	14 404.00	3581.7	8.6
44	10 946.40	3336.6	11.6	116	14 078.00	3470.0	8.5
45	12 155.10	3948.1	12	117	14 050.00	3725.3	9.5
46	15 131.20	4916.3	10.9	118	12 815.40	3620.4	9.7
47	13 952.20	4574.5	10.9	119	14 606.70	4232.8	8.7
48	11 503.40	3517.2	10.6	120	15 485.10	4436.5	8.6
49	14 077.00	4848.2	12.2	121	14 484.20	3007.3	5.3
50	11 212.90	3564.6	11.5	122	15 480.10	2850.4	4.7
51	16 252.80	3952.3	8.5	123	15 552.00	2842.3	4.3
52	16 070.70	4557.3	9.5	124	15 782.60	3411.2	5.3

Table 7. Predicted forces on cutter-head under certain circumstances

Rock type	UCS /MPa	Penetration P/(mm • r^{-1})	Cutterhead estimated force/MN	Cutter estimated force/kN
Igmatitic granite	80	12	9.61	149
	122	9	15.4	239
	153	4	15.9	248
	192	2	17.2	267

As shown in Fig. 11, SE(Eq. (19)) decreases with increasing depth of cutter, which means under certain geological conditions, large penetration tunneling is more likely to enhance the efficiency of TBM tunneling, and to achieve fast and efficient tunneling.

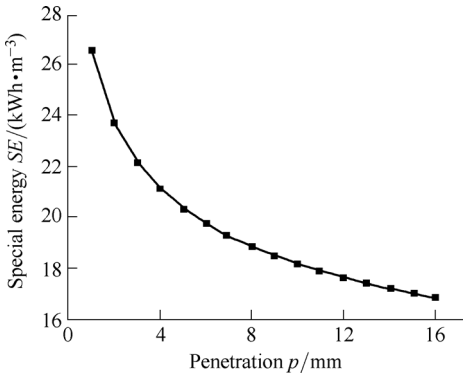

Fig. 11. Effect of penetration depth on specific energy

3.2 Analysis of cutter-head thrust and torque

Fig. 12 shows comparison of predicted thrust and onsite data[17] in Qinling Tunnel. Assuming rock UCS ranges from 50 MPa to 200 MPa, the shadow shows predicted thrust range, and the small squares represent the record data in Qingling Tunnel. According to Fig. 12, TB880E can break rock at high speed when the UCS ranges from 50 to 140 MPa, but when the rock becomes hard, penetration decreases and the driving speed reduces. Fig. 13 shows the comparison between predicted torque and actual measured values in the same way.

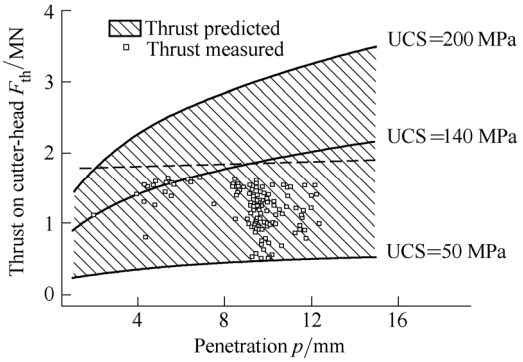

Fig. 12. Comparison of Thrust prediction and in site record

Compare Fig. 12 to Fig. 13, when the rock UCS value is 200 MPa, the rated thrust satisfies penetration about 2mm, while the rated torque satisfies tunneling penetration above 4mm. when the rock UCS is 140 MPa, the rated thrust satisfies penetration about 10mm, while the rated torque only satisfies tunneling penetration about 8 mm. In conclusion, when the UCS is high and the tunneling is at a low speed, the thrust may be insufficient. When the tunneling is at a high speed, the torque will be a limiting factor for increasing of tunneling speed.

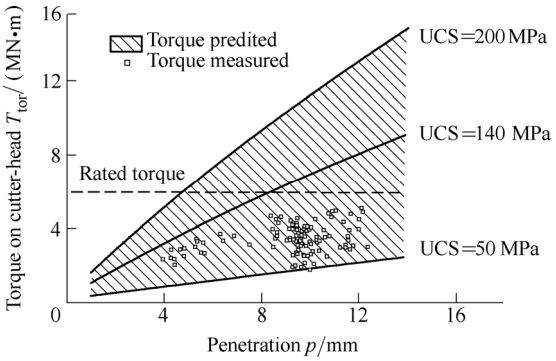

Fig. 13. Comparison of Torque predicted and in site record

3.3 Relationship between ZT and penetration

Thrust and torque on the cutter-head are two most important values for TBM design, and the relationship between them in the process of excavating can be expressed as follows:

$$ZT = \frac{T_{\text{tor}}}{F_{\text{th}}} = \frac{\sum_{i=1}^{n} F_{\text{ri}} \cdot r_i}{\sum_{i=1}^{n} F_{\text{v}i}}, \tag{24}$$

$$ZTI = \frac{ZT}{p}. \tag{25}$$

Fig. 14 shows the approximate linear relationship between ZT and penetration. As the penetration increases, the growing rate of the torque is greater than the thrust. Therefore, keeping the right tunneling parameters in the process of TBM tunneling is very important, and the relationship between p and ZT varies with the cutters' arrangement on the cutter-head.

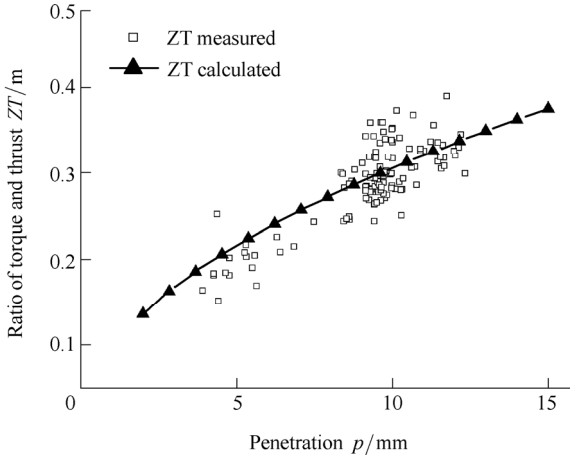

Fig. 14. Relationship between p and ZT on TB880E

Data in Fig. 14 shows that using cutter-head load model to estimate the relationship is an effective way to enhance the accuracy of the operation and tunnel high-efficiency.

4 Conclusions

(1) A cutter-head load model is established by using CSM prediction model, which can be used to study force distribution on cutter-head and the relationship between thrust and penetration in certain geologies.

(2) A general principle of disc cutters' layout design is proposed. When putting cutters at central, the limiting of the load and the largest rock breaking spacing is considered, when arranging in the outer ring cutters abrasion is the main consideration and outer circle cutters spacings are smaller or arranged several cutters on one trace..

(3) Thrust and torque characteristics of TB880E are analyzed and validated with TB880E record data. At different geological conditions, with the growth of rock UCS, cutter-head need more thrust than torque.

(4) A fitting mathematical model of ZT and penetration is established.

References

[1] ROSTAMI J, OZDEMIR L. A new model for performance prediction of hard rock TBMs[C]//*Proceedings of the Rapid Excavation and Tunneling Conference*, Boston, America, June 13–17, 1993: 793–793.

[2] LI Gang, ZHU Lida, YANG Jianyu, et al. A method to predict disc cutter wear extent for hard rock TBMs based on CSM model[J]. *China Mechanical Engineering*, 2014, 25(1): 32–35. (in Chinese)

[3] LI Gang, YU Tianbiao, FEI Xueting, et al. A method to predict cutterhead specific energy for TBM based on CSM model[J]. *Journal of Northeastern University(Natural Science)*, 2012, 33(1): 1766–1769. (in Chinese)

[4] ZHANG Zhaohuang, QIAO Yongli. Research on the layout of TBM disc cutter[J]. *Engineering Mechanics*, 2011, 28(5): 172–177. (in Chinese)

[5] HUO Junzhou, SUN Wei. Optimal disc cutters plane layout design of the full-face rock tunnel boring machine based on a multi-objective genetic algorithm[J]. *Journal of Mechanical Science and Technology*, 2010, 24(2): 521–528.

[6] HUO Junzhou, SUN Wei. Coupling layout design of disc cutters group and cutterhead supporting structure[J]. *Journal of Mechanical Engineer*, 2014, 50(21): 23–30. (in Chinese)

[7] ZHANG Zhaohuang, MENG Liang, SUN Fei. Wear analysis of disc cutters of full face rock tunnel boring machine[J]. *Chinese Journal of Mechanical Engineering*, 2014, 27(6): 1294–1300.

[8] ZHANG Zhaohuang, MENG Liang, SUN Fei. Rock deformation equations and application to the study on slantingly installed disc cutter[J]. *Acta Mechanica Sinica*, 2014, 30(4): 540–546.

[9] GUO Wei, HU Jing, WANG Lei, et al. Study on the opening distribution characteristics of earth pressure balance shield cutter head based on CFD[J]. *Journal of Mechanical Engineering*, 2012, 48(17): 144–151. (in Chinese)

[10] GUO Wei, HU Jing, LIU Jianqin. Analysis of soil of excavation face with shield cutter head based on computational fluid dynamics[J]. *Journal of Tianjin University*, 2012, 45(12): 1039–1044.

[11] SAFFET Y. Utilizing rock mass properties for predicting TBM performance in hard rock condition[J]. *Tunnellng and Underground Space Technology*, 2008, 23: 326–339.

[12] ROSTAMI J, OZDEMIR L, NILSON B. Comparison between CSM and NTH hard rock TBM performance prediction models[C]// *Proceedings of Annual Technical Meeting of the Institute of Shaft Drilling Technology*, Las Vegas, America, Sept 17–19, 1996: 1–10.

[13] ROXBOROUGH F F, PHILLIPS H R. Rock excavation by disc cutter[J]. *International Journal of Rock Mechanics and Mining Sciences*, 1975, 12(12): 361–366.

[14] SANIO H P. Prediction of the performance of disc cutters in anisotropic rock[J]. *International Journal of Rock Mechanics and Mining Sciences*, 1985, 22(3): 153–161

[15] XIA Yimin, OUYANG Tao. Mechanical model of breaking rock and force characteristic of disc cutter[J]. *Journal of Central South University*, 2012, 19(7): 1849–1852.

[16] ZHANG Zhanghuang, MENG Liang, SUN Fei. Design theory of full face rock tunnel boring machine transition cutter edge angle and its application[J]. *Chinese Journal of Mechanical Engineer*, 2013, 26(3): 541–546.

[17] PENG D. TBM construction at the output of No.1 Qinling tunnel on Xikang railway[J]. *Modern Tunnelling Technology*, 2001, 38(6): 33–37. (in Chinese)

[18] ENTACHER M, WINTER G, GALLER R. Cutter force measurement on tunnel boring machines—Implementation at Koralm tunnel[J]. *Tunnelling and Underground Space Technology*, 2013, 38(1): 487–496.

[19] CHO J, JEON S, JEONG H, CHANG S. Evaluation of cutting efficiency during TBM disc cutter excavation within a Korean granitic rock using linear-cutting-machine testing and photogrammetric measurement[J]. *Tunnelling and Underground Space Technology*, 2013, 35(1): 37–54.

[20] ZHANG H. Study on numerical simulations of performance of tunnel boring machines[J]. *Tunnel Construction*, 2007, 26(supp): 1–7. (in Chinese)

[21] WANG L. The energy method to predict disc cutter wear extent for hard rock TBMs[J]. *Tunnelling and Underground Space Technology*, 2012, 28(1): 183–191.

Biographical notes

LIU Jianqin, born in 1972, is currently an associate professor and a master supervisor at *School of Mechanical Engineering, Tianjin University, China*. Her research interests include mechanism dynamics and design of mechanisms, etc.
Tel: +86-13516187323; E-mail: liujianqin@tju.edu.cn

REN Jiabao, born in 1990, is currently a PhD candidate at *Key Laboratory of Mechanism Theory and Equipment Design of Ministry of Education, Tianjin University*. His research interests include TBM cutter-head design and product design, etc.
Tel: +86-15022695926; E-mail: renjiabao@tju.edu.cn

GUO Wei, born in 1965, is currently a professor and a doctor supervisor at *School of Mechanical Engineering, Tianjin University, China*. His research interest is product digitital design.